

Naval Research Laboratory

Washington, DC 20375-5320



NRL/MR/5310--97-8378

Hybrid Version of Method of Moments Computer Code: IBC3D

DOUGLAS TAYLOR

*Radar Analysis Branch
Radar Division*

May 20, 1999

19990518 011

Approved for public release; distribution unlimited.

REPORT DOCUMENTATION PAGE

*Form Approved
OMB No. 0704-0188*

Public reporting burden for this collection of information is estimated to average 1 hour per response, including the time for reviewing instructions, searching existing data sources, gathering and maintaining the data needed, and completing and reviewing the collection of information. Send comments regarding this burden estimate or any other aspect of this collection of information, including suggestions for reducing this burden, to Washington Headquarters Services, Directorate for Information Operations and Reports, 1215 Jefferson Davis Highway, Suite 1204, Arlington, VA 22202-4302, and to the Office of Management and Budget, Paperwork Reduction Project (0704-0188), Washington, DC 20503.

1. AGENCY USE ONLY (Leave Blank)			2. REPORT DATE May 20, 1999		3. REPORT TYPE AND DATES COVERED				
4. TITLE AND SUBTITLE Hybrid Version of Method of Moments Computer Code: IBC3D			5. FUNDING NUMBERS PE - 61153N EW21-05-43						
6. AUTHOR(S) Douglas J. Taylor									
7. PERFORMING ORGANIZATION NAME(S) AND ADDRESS(ES) Naval Research Laboratory Washington, DC 20375-5320			8. PERFORMING ORGANIZATION REPORT NUMBER NRL/MR/5310--99-8378						
9. SPONSORING/MONITORING AGENCY NAME(S) AND ADDRESS(ES) Office of Naval Research Arlington, VA 22217									
10. SPONSORING/MONITORING AGENCY REPORT NUMBER									
11. SUPPLEMENTARY NOTES									
12a. DISTRIBUTION/AVAILABILITY STATEMENT Approved for public release; distribution unlimited.				12b. DISTRIBUTION CODE A					
13. ABSTRACT (Maximum 200 words) IBC3D is a computer program used to calculate the electromagnetic scattering cross section and electric/magnetic surface currents for arbitrary 3-dimensional bodies coated with anisotropic lossy materials. An enhanced version of this code, developed by the Radar Division of the Naval Research Laboratory (NRL), is described here that allows one to generate a hybrid scattering solution by incorporating surface currents generated external to the IBC3D. The benefit derived from using the hybrid approach is gained by reducing the number of surface current unknowns required to produce a scattering cross section using numerically intensive computer codes such as IBC3D. When compared to the unmodified IBC3D solution for a 5-sided prism shaped object a 20 percent reduction in the number of electric surface current unknowns was obtained using the hybrid version of the code with minimal sacrifice in accuracy.									
14. SUBJECT TERMS Radar cross section Hybrid method				15. NUMBER OF PAGES 22		16. PRICE CODE			
17. SECURITY CLASSIFICATION OF REPORT UNCLASSIFIED						18. SECURITY CLASSIFICATION OF THIS PAGE UNCLASSIFIED		19. SECURITY CLASSIFICATION OF ABSTRACT UNCLASSIFIED	

CONTENTS

INTRODUCTION	1
THEORY	1
NUMERICAL IMPLEMENTATION	4
COMPARISON WITH ANALYTICAL, MEASURED DATA	5
CONCLUSIONS	9
REFERENCES	11

HYBRID VERSION OF METHOD OF MOMENTS COMPUTER CODE: IBC3D

INTRODUCTION

The underlying computational engines for computer simulation of electromagnetic wave scattering are routinely classified into two fundamentally different approaches, high frequency and low frequency. The low frequency approaches are based on strictly numerical methods that generate scattering simulations from numerical solutions to partial differential equations or integral equations formulated from Maxwell's equations. The high frequency approaches are based on asymptotic solutions to Maxwell's equations based on assumptions about the nature of the wave-object interaction. The strengths and weaknesses of these two approaches can be summarized in terms of an object's electrical dimension. The low frequency methods provide accuracy but consume computer resources (memory, cpu time, disk space) at a very rapid rate as the frequency increases. As a result the low frequency methods are limited to the available computer resources and become prohibitive for electrically large objects. The high frequency methods suffer from an opposite constraint, they lose accuracy as the electrical size of the object becomes small but provide accurate results for electrically large objects.

A method that combines the two approaches in a manner that appears to bridge this gap between the high and low frequency methods is a hybrid physical optics method of moments (PO/MoM) combination [1,2]. The hybrid PO/MoM approach published by Putnam and Medgyesi-Mitschang is general enough to allow the modification of an existing 3-dimensional method-of-moments numerical scattering computer program into a hybrid code capable of using externally generated scattering currents as part of the numerical solution. The Radar Division of NRL utilized the Putnam and Medgyesi-Mitschang analysis to convert the IBC3D code into a hybrid code for research into hybrid scattering methods.

THEORY

The mathematical foundation of the hybrid IBC3D code is a simple extension of the formulation of the original IBC3D computer code. In the original code, electric surface currents were solved for numerically. In the hybrid code, surface currents on portions of

Manuscript approved April 9, 1999.

the scattering geometry are considered to be known quantities and are isolated from the currents to be solved for numerically. The following paragraphs give a summary of how this is implemented to produce the hybrid IBC3D code.

The original version of IBC3D was developed to provide a numerical scattering solution for coated bodies of arbitrary shape using triangular surface patch elements and an anisotropic impedance boundary condition (IBC) to model the coatings [3]. The numerical formulation of the original IBC3D code is the electric field integral equation (EFIE) which is solved using a Galerkin MoM technique. Their formulation specified that on the surface of the scattering body the following integral relation between the incident field $\vec{E}_{\text{tan}}^{\text{inc}}(\vec{r})$, the surface impedance \vec{Z}_s and the equivalent induced currents $\vec{J}(\vec{r})$ holds:

$$\begin{aligned}\vec{E}_{\text{tan}}^{\text{inc}}(\vec{r}) = & [j\omega\mu \int_S \vec{J}(\vec{r}') G(\vec{r}', \vec{r}) dS' + \frac{1}{\epsilon} \nabla \int_S \sigma(\vec{r}') G(\vec{r}', \vec{r}) dS' + \frac{1}{2} \eta (\vec{Z}_s \cdot \vec{J}) \\ & + \int_S \eta \{ \hat{n}' \times (\vec{Z}_s \cdot \vec{J}) \} \times \nabla G(\vec{r}', \vec{r}) dS']_{\text{tan}}.\end{aligned}\quad (1)$$

The surface charge $\sigma(\vec{r})$ is eliminated by expressing it in terms of the current $\vec{J}(\vec{r})$ using the equation of continuity, $G(\vec{r}, \vec{r})$ is the free space Greens function, \hat{n} is the surface normal and η is the impedance of free space. Equation (1) re-written in compact operator notation is

$$L(\vec{J}) = \vec{E}_{\text{tan}}^{\text{inc}}. \quad (2)$$

This integral equation is solved by first expanding the unknown currents, \vec{J} , in terms of basis functions,

$$\vec{J} = \sum_{n=1}^N I_n \vec{f}_n(r), \quad (3)$$

where I_n is the amplitude of the current basis function $\vec{f}_n(r)$, Rao-Wilton-Glisson (RWG) triangular rooftop basis functions are used in IBC3D. Employing the Galerkin method to generate the following inner products generates a system of linear equations

$$\langle g_m, L(\vec{J}) \rangle = \langle g_m, \vec{E}_{\text{tan}}^{\text{inc}} \rangle. \quad (4)$$

This system of linear equations, re-written using standard notation,

$$\sum_{n=1}^N Z_{mn} I_n = V_m , \quad (5)$$

where $Z_{mn} = \langle g_m, L(\vec{f}_n(\vec{r})) \rangle$ and $V_m = \langle g_m, \vec{E}_{\tan}^{inc} \rangle$, is solved numerically in IBC3D using LUD factor and solve routines from the Linpack library [5].

The purpose of the hybrid formulation is to reduce the size of the matrix equation corresponding to Eq. (5) that arises in the IBC3D solution. This is accomplished by assuming that \vec{J} can be represented accurately with a known current distribution in selected regions. In the case of the PO/MoM hybrid, a physical optics current distribution is assumed in the lit region:

$$\vec{J} = \begin{cases} \vec{J}(\vec{r}) = \sum_{n=1}^N I_n \vec{f}_n(\vec{r}), & \vec{r} \in \text{Numerical region} \\ \vec{J}^{PO}(\vec{r}) = 2\hat{n} \times \vec{H}^{inc}(\vec{r}), & \vec{r} \in \text{Lit, PO region} \end{cases} . \quad (6)$$

The impact of this can be understood by noting that Eq. (4) is an expression of the boundary condition $\vec{E}_{\tan}^{total} = 0$ over the region spanned by the testing basis function g_m . There are three contributors to the field in this region: the incident field, the field produced by the unknown currents and the field produced by the physical optic currents. Isolating the unknown currents from the known quantities by rearranging Eq. (4) results in the following set of equations,

$$\langle g_m, L(\vec{J} + \vec{J}^{PO}) \rangle = \langle g_m, L(\vec{J}) + L(\vec{J}^{PO}) \rangle = \langle g_m, \vec{E}_{\tan}^{inc} \rangle , \quad (7)$$

$$\langle g_m, L(\vec{J}) \rangle = \langle g_m, \vec{E}_{\tan}^{inc} \rangle - \langle g_m, L(\vec{J}^{PO}) \rangle . \quad (8)$$

If the PO currents are expanded using the same basis functions as the unknown currents,

$$\vec{J}^{PO}(\vec{r}) = \sum_{j=1}^M I_j^{PO} \vec{h}_j(\vec{r}) \text{ where } I_j^{PO} \text{ is the amplitude of the physical optic current, then Eq.}$$

(8) produces a system of linear equations, when written in standard notation,

$$\sum_{n=1}^{N-M} Z_{mn} I_n = V_m - \sum_{j=N-M+1}^N Z_{mj} I_j^{PO} , \quad (9)$$

that describe the implementation of the PO/MoM hybrid. The benefit of this implementation results from reducing the order of the matrix equation that needs to be solved. Equation (9) describes the solution of a problem that has been reduced from

order N to order $N-M$ by substituting M PO currents into the problem. The influence of the PO currents on the unknown currents is clear from Eq. (9). The right hand side of Eq. (9) contains the incident field plus the fields radiated by the PO currents into the remaining numerical regions, this has a direct effect on the solution of the current unknowns on the left-hand side of the equation. Equation (9) is the hybrid PO/MOM implementation described by Putnam and has been incorporated in the computer code IBC3D at NRL.

The expansion coefficients of the PO currents in the RWG basis functions are constructed in the following approximate manner, as outlined by Putnam [1]. The PO current amplitude for edge k is computed using either triangular facet, T_k^+ or T_k^- , and the incident magnetic field $\vec{H}^{inc}(\vec{r})$, specifically,

$$I_k^{PO} = \begin{cases} -2\hat{p}_k^+ \cdot \vec{H}^{inc}(\vec{r}), & \vec{r} \in T_k^+ \\ +2\hat{p}_k^- \cdot \vec{H}^{inc}(\vec{r}), & \vec{r} \in T_k^- \end{cases}, \quad (10)$$

where the unit vectors \hat{p}_k^\pm are parallel to edge k and are given by

$$\hat{p}_k^\pm = \hat{n}^\pm \times \hat{u}_k^\pm, \quad (11)$$

the cross product of the normals \hat{n}^\pm to the triangular patch and unit vectors \hat{u}_k^\pm that are normal to the edge k and lie in the plane of the triangular facets T_k^\pm . These calculations are performed external to the modified, hybrid version of IBC3D and only the current amplitudes of Eq. (10), are used in IBC3D.

NUMERICAL IMPLEMENTATION

The hybrid version of IBC3D has left most of the original code structure and input files intact. In the original code, the program read a parameter file as input that described the frequencies, polarization, source and receiver locations and geometry file to be used in the calculation. The geometry file contains the triangular surface patch model of the object. This geometry file contains the points, edges and triangular facets that form the surface mesh. The points, edges and facets are numbered sequentially and this information is used in IBC3D to facilitate the computation.

The process of filling the impedance matrix is accomplished in IBC3D by looping over the triangular facets that form the model. Two nested loops are used, one for the source facet and the other for the field facet. The current unknowns in the impedance matrix equation, Eq. (5), use the edge numbers from the geometry file as array indices. Each facet index has a corresponding triplet of edge numbers that are used to direct impedance matrix calculations to their proper position in the impedance matrix array.

The hybrid version of IBC3D maintains this same organization but with additional logic to accommodate the fact that there are now two different types of current unknowns. In addition to the geometry and parameter files as input, a file containing the facet numbers selected for PO currents and a file containing the complex PO current amplitude for the PO edges are required. These files are created external to IBC3D using a separate program to process the geometry file.

The internal logic used to fill the impedance matrix is modified to account for the presence of the PO currents that radiate into the numerical MoM region. This logic is based on the nature of the source and field edges in the nested double loop inside the IBC3D program that fills the impedance matrix. This logic can be simply explained in terms of the characteristics of the source and field edges. Ordinarily, the source and field edges are both MoM and the computation performed in the loop is added to the impedance matrix. If the source edge is PO and the field edge is MOM, then this result is multiplied by the source edge PO current and the product is added to the right hand side voltage vector. If the source and field edges are both PO or the source edge is MOM and the field edge is PO, no calculation is performed.

Along boundaries between PO and MoM regions there are instances where PO and MOM facets share a common edge. When this occurs the edge is labeled a PO edge by default. This choice simplified the logic described above.

COMPARISON WITH ANALYTICAL, MEASURED DATA

The hybrid version of IBC3D described here joins together the numerical MoM method that IBC3D is based on with asymptotic physical optics currents. The accuracy of the code, using both the traditional MoM only approach and the hybrid method, is

demonstrated here by comparing with the Mie series solution for a metal sphere and radar cross section range measured data for a simple geometrical shape.

The Mie series solution for electromagnetic wave scattering from a PEC (perfect electric conductor) sphere allows direct comparison of the PO current approximation with the exact currents for this geometry. The equivalent electric currents, computed by calculating $\hat{n} \times H^{total}$ on the sphere's surface, are shown in Figure 1. The physical optics approximation, $J_{EPlane}^{PO} = 2$ and $J_{HPlane}^{PO} = 2\cos(\varphi)$, of the electric currents are also shown in Figure 1. The exact current and the physical optic current can be seen to agree out to about 45 degrees for this particular sphere with an electrical size of $ka = 4.2$. The agreement decays rapidly beyond 45 degrees and is poor at the terminator between the lit and shadowed portion of the sphere surface.

The result of using three different methods to compute the monostatic backscatter of the PEC sphere is shown in Figure 2. In this figure the Mie series solution, the purely numerical IBC3D MoM result, and the hybrid PO/MoM solutions are plotted for comparison. The strictly numerical MoM solution provides a result that agrees well with the Mie series solution for $0.4 < ka < 4.2$. The hybrid PO/MOM solution shown in Figure 2 employed different numbers of PO currents in the solution. The hybrid solution is not appropriate for low ka values, but appears to produce more accurate answers as the sphere's electrical size increases.

The selection of which edges in the sphere's mesh model used physical optics currents was based on the orientation of each triangular facet with respect to the incident plane wave. The angle between the facet normal and the incident wave direction was calculated, and if it was less than a prescribed value, then the unknowns associated with the three edges forming that triangle were selected to be represented with physical optics currents. This angle limit was set to 15 degrees in one instance and 45 degrees in another to gauge the effect of increasing the number of physical optics currents on the calculated backscatter cross section. The sphere's numerical mesh contains 699 edges or unknowns in total, with a facet limit of 15 degrees, 103 of these unknowns were replaced with physical optic currents. When the facet limit was increased to 45 degrees, 256 of the unknowns were replaced with physical optic currents.

The surprising result is that the hybrid calculated backscatter agrees with the Mie series result in the low ka region. In the frequency region $ka < 1$ the physical optic currents are a very poor approximation to the exact currents on the sphere, nonetheless the calculated backscatter returns agree. The reason for this is not clear, but in general the physical optic currents should only be substituted in regions that are electrically large.

The sphere is a complicated scatterer with a combination of specular and surface wave modes that constructively or destructively interfere to produce the peaks in the backscatter spectrum. The ability of the hybrid method, relying on specular physical optic currents, to reproduce these features generally degrades as more physical optic currents are substituted into the hybrid calculation, because the physical optics currents do not contain the surface wave physics required to represent the scattering accurately.

The sphere provides an excellent reference solution that can be calculated using a series expansion to produce an exact answer for comparison. However, it is not a realistic or interesting object for practical reasons. A simple object that was constructed and tested for radar scattering provided a more realistic test case for the hybrid method. The object is prism shaped, referred to here as Prism V20, with 5 sides and is described in NRL Memorandum Report 6247 [4]. The physical dimensions of the Prism V20 model are given in Figure 3.

The numerical mesh model of the Prism V20 object is shown in Figure 3. The mesh contains 724 points and 1,444 triangular facets that translate into 2,166 electric current unknowns. The monostatic cross section calculated using the unmodified IBC3D computer code is plotted in Figure 4 along with the measured cross section at 432 MHz. The scattering from the PrismV20 object can be summarized as arising from specular returns from the large flat faces of the model mixed with the edge waves and diffraction from the sharp edges of the model. The good agreement between the measured and calculated cross sections of Figure 4 confirm that the purely numerical solution is faithfully simulating these scattering mechanisms.

The hybrid version of IBC3D cannot decide on its own when to use PO currents and when not to, this decision is made external to the code. The natural decomposition of the Prism V20 object into numerical (MOM) regions and physical optics (PO) regions is shown in Figure 5. In this figure the edges and corners of the model have been reserved

for the strictly numerical method. The large flat areas utilize the PO currents if the flat areas are directly illuminated by the incident wave. No angular limit was placed on the orientation of the facets to be selected as a PO facet, unlike the hybrid sphere calculations.

It is important to emphasize here that the PO and MoM regions of the V20 prism object are coupled in the hybrid calculations. The scattering cross section calculated using the hybrid method is *not* simply the sum of the PO returns from the flat areas in Figure 5 with the returns from the edges and corners using the MoM method. Instead the MoM method applied to the edges and corners ‘feels’ the presence of the large flat PO areas via the radiated near fields generated by the PO currents. The coupling of the PO region to the MoM region is essential to enhance the accuracy and utility of the hybrid method.

The measured cross section and hybrid method calculated cross section are plotted in Figure 6. The hybrid calculation produces accurate cross sections in the neighborhood of the large specular returns at 270, 140 and 70 degrees. In these regions, the scattering is dominated by the large reflection from the flat faces, and is accurately approximated with the physical optic currents. The large amplitude feature centered near 200 degrees is a non-specular feature produced by an edge wave travelling along the long face of the Prism V20 body. The feature is faithfully predicted by the hybrid method employed here. It is significant that this feature has been calculated correctly because it is an important scattering mechanism that is not predicted using physical optic currents alone.

A small feature that appears in the measured cross section between 210 and 220 degrees is underestimated by the hybrid method. The source of this discrepancy appears to be the use of the PO currents on the short face of the Prism V20 object. In the 180 to 220 degree region the short face is oriented at a very shallow angle, grazing incidence, relative to the incident wave and the PO current approximation is likely a poor one in this situation. At 220 degrees the short face exits the lit region and the currents on the face change from PO to numerical MOM, which results in a jump in the calculated cross section that matches the measured cross section.

The measured and calculated cross section both show a deep narrow null at 180 degrees. This null is the result of destructive interference between edge waves on the

longest face and shortest face of the Prism V20 geometry. The hybrid method using PO currents on the short face and either numerical or PO currents on the long face reproduce this effect, although the cancellation is not to the same level as in the measured cross section. The large, broad feature around 0 degrees is apparently of the same nature, two edge waves travelling down the longest and second longest faces of the Prism V20 object. However, the hybrid method employed here does not reproduce the shape and amplitude of the large feature centered about 0 degrees. The phasing of the edge waves on the two edges is not correct and results in reduced amplitude. This scattering feature appears to be largely independent of the number of PO currents used on the two faces.

Figure 7 shows the number of PO unknowns used in the hybrid calculation as a function of incidence angle. The greatest number occurs when the two largest faces, ‘a’ and ‘b’, are lit simultaneously. This occurs between 340 and 0 degrees. The smallest number of PO unknowns occurs between 160 and 180 degrees when only face ‘c’ is lit. Recall that the total number of current unknowns for the Prism V20 object is 2,166, and depending on the incidence angle, between 106 and 723 were selected for PO currents. The average over the full 360 degrees was 410 PO current unknowns. This is approximately 20 percent of the total number of unknowns in the problem.

CONCLUSION

The theme of this hybrid method is to join together two areas of research, namely high and low frequency electromagnetic methods, which traditionally have worked independent of one another. The reason for wanting to accomplish such a task is that there exists a large class of electromagnetic simulation problems for which no computer solution has been found to be acceptable. Typical of this class are reduced signature military platforms, conformal embedded antenna systems and electromagnetic interference simulation. High fidelity simulations usually require low frequency, numerical methods. Unfortunately, the strictly numerical methods will never arrive at an answer for many problems in this class because of the extraordinary computational demands required to produce a solution. On the other hand, the high frequency,

asymptotic, methods presented with the same class of problems can produce solutions but are likely to be incorrect because the scattering physics is incomplete.

The hybrid method described here joins together high and low frequency methods in a manner that preserves their strengths and minimizes their shortcomings. Improvements in the implementation of the hybrid method could be realized in the following areas:

1. The expansion of currents in RWG basis functions is cumbersome for currents external to IBC3D. Implementing a PO/MOM hybrid based on the direct evaluation of fields produced by these currents makes the method more flexible and general by evaluating the right hand side of Eq. 8 in a more natural manner.
2. Utilize fast methods for the remaining MOM portion, such as fast multipole method (FMM) or adaptive integral method (AIM). The benefit of this is obvious.
3. A great many more unknowns could be eliminated if expressions were available to describe accurately the currents in the shadowed region. With perhaps one half of an object not directly illuminated, these regions must remain purely numerical and therefore become ultimately a limiting factor. It may be possible that some currents could be set to zero deep in the shadowed region.
4. Devise a strategy to eliminate the abrupt changes in the number of unknowns as a function of incidence angle (see Figure 7). This is especially noticeable when large flat regions make the transition from darkness to being illuminated.
5. Expand the application of this hybrid method by employing alternate analytical current solutions. This could be accomplished by augmenting the physical optics currents with application specific current distributions, for example, currents on coated edges calculated using NRL's Hybrid Theory of Diffraction [6], and currents from infinite periodic array moment method codes could be used to solve a finite-size frequency-selective surface problem.

REFERENCES

1. L.N. Medgyesi-Mitschang and J.M. Putnam, "Hybrid formulation for arbitrary 3D bodies", Proceedings of the Tenth Annual Review of Progress in Applied Computational Electromagnetics, p. 267-74 vol. 2, Appl. Comput. Electromagnetics Soc; Monterey, CA, 21-26 March 1994
2. U. Jakobus and F. M. Landstorfer, "Current-based hybrid moment analysis of electromagnetic radiation and scattering problems," ACES Journal, vol. 10, pp. 38-46, Nov. 1995. Special Issue on Advances In the Application of the Method of Moments to Electromagnetic Radiation and Scattering Problems.
3. F. Falco, D. Koppel, N. Erlbach and M. Orman "IBC3D Anisotropic Impedance Boundary Condition 3D Scattering Code", Vol. 1, User's Manual and Programmer's Guide. Riverside Research Institute, New York, New York. November, 1991.
4. B. L. Merchant, W. P. Pala, H. J. Bilow, F. J. Rachford, C. A. Carosella and D. J. Taylor, "Measurement Program SS04 Results (U)", October 1989, NRL Memo Report 6247. (Classified)
5. J. J. Dongarra, C. B. Moler, J. R. Bunch and G. W. Stewart, "LINPACK Users' Guide", Society for Industrial and Applied Mathematics, Philadelphia, Pennsylvania, 1979.
6. H. J. Bilow, "Scattering by an Infinite Wedge with Tensor Impedance Boundary Conditions - A Moment Method/Physical Optics Solution for the Currents". IEEE Transactions on Antennas and Propagation 39:767-773, April 24, 1991.

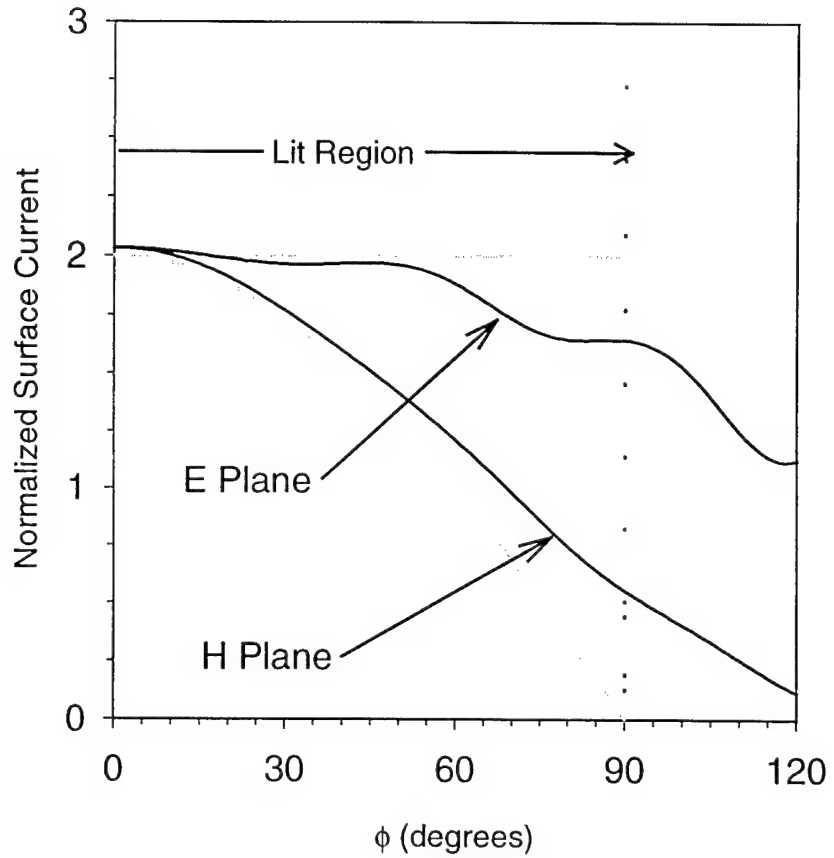


FIGURE 1. Electric surface current on a perfectly conducting sphere, $ka = 4.2$, along a line parallel to the incident electric field (E Plane) and magnetic field (H Plane). The Mie series is used to calculate \vec{J} from $\hat{n} \times \vec{H}_{total}$ on the surface the sphere and is plotted using solid lines. The physical optics approximation, $J_{E\text{ Plane}}^{\text{PO}} = 2$ and $J_{H\text{ Plane}}^{\text{PO}} = 2\cos(\phi)$, is plotted with dashed lines. The dotted line indicates the position of the transition from the lit region to the shadowed side of the sphere. The surface current has been normalized to the magnitude of the incident magnetic field.

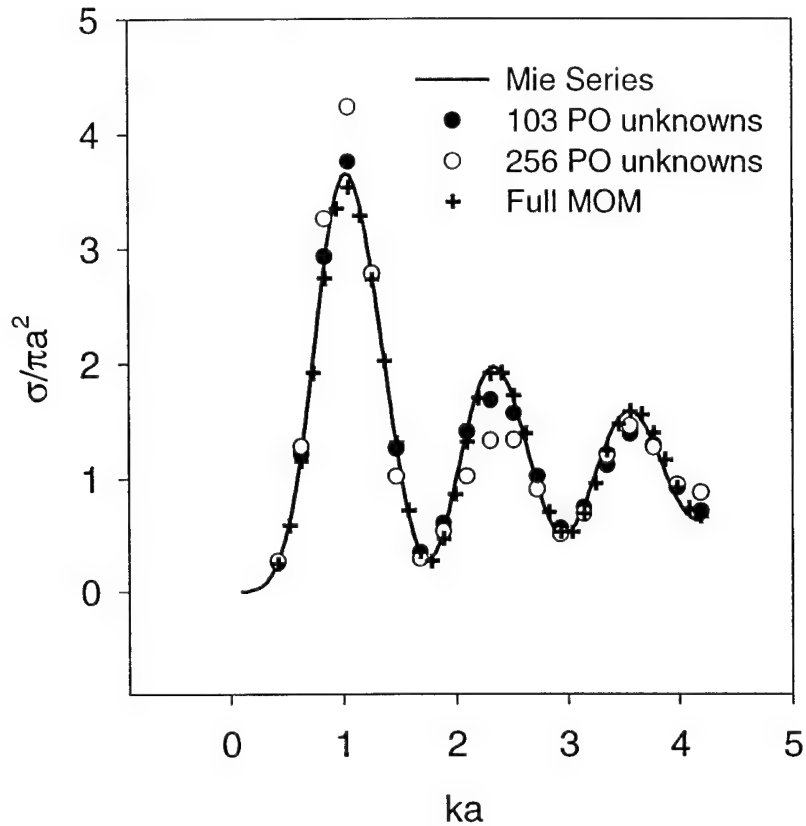


FIGURE 2. Monostatic cross section of a PEC sphere computed using exact Mie series solution and the hybrid PO/MOM approach. Two different hybrid results are shown which represent different numbers of PO currents in the hybrid solution. The sphere was modeled using triangular patches, and a patch was assigned PO currents based on its orientation with respect to the incident field. In this figure limits of 15 and 45 degrees are used to produce the two sets of data. The full MOM solution with 699 unknowns is also plotted for comparison to the hybrid and exact results.

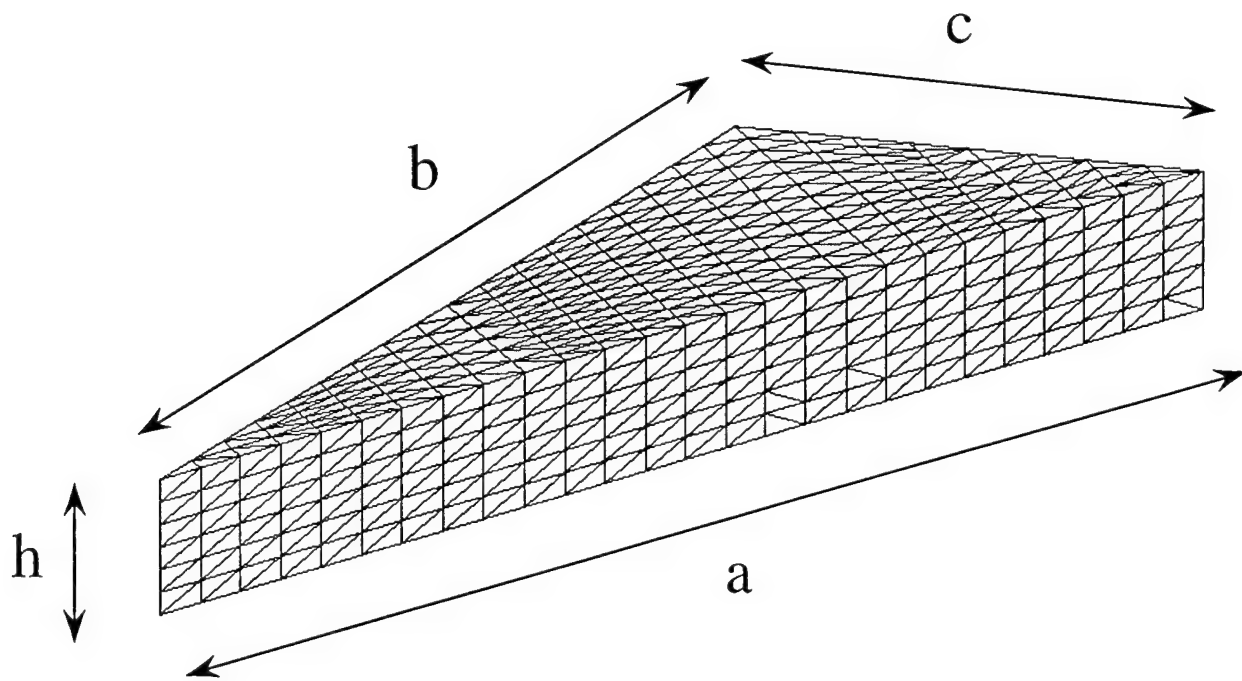


FIGURE 3. Numerical mesh model of the Prism V20 geometry as used with the hybrid PO/MOM version of the IBC3D computer code. Dimensions of the actual model are: $a = 2.40$ m, $b = 1.78$ m, $c = 0.95$ m and $h = 0.30$ m. The corners of the object form a triangle with 20° , 40° and 120° angles.

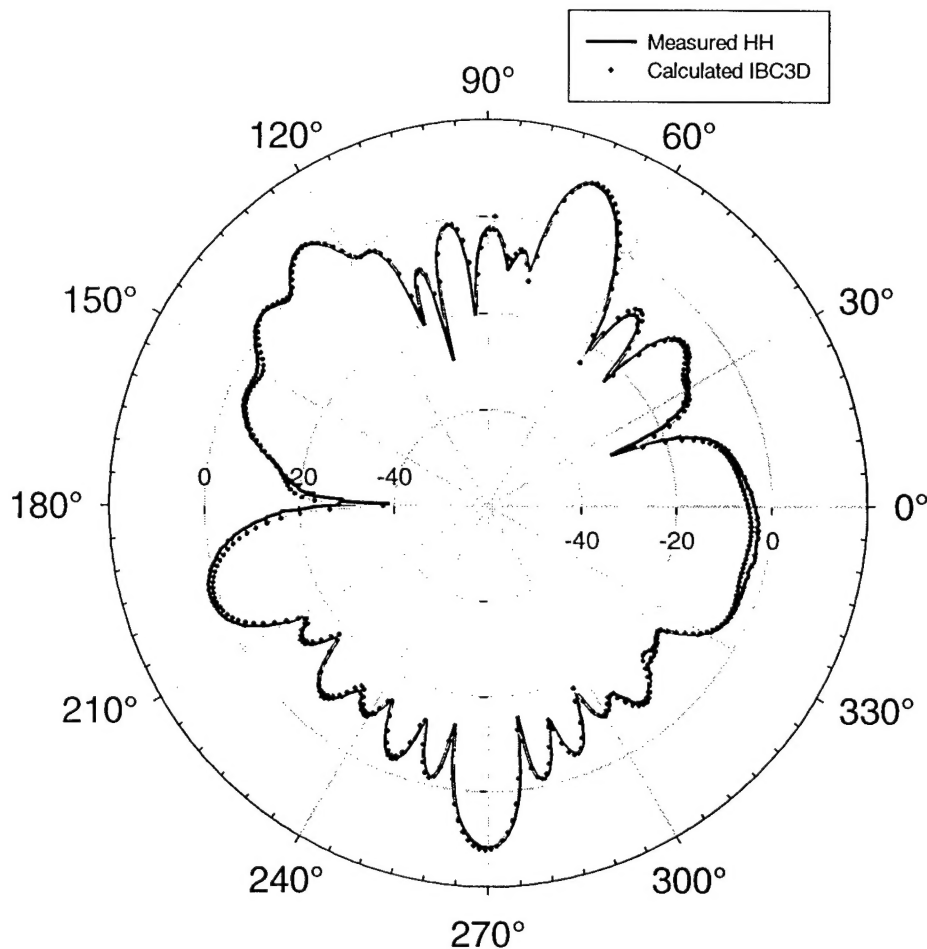
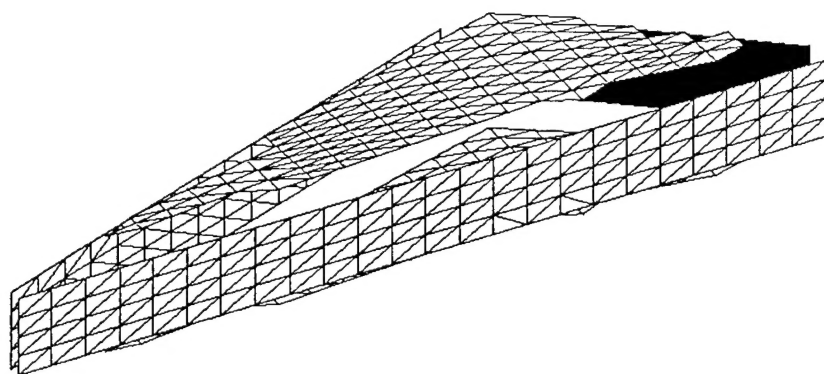
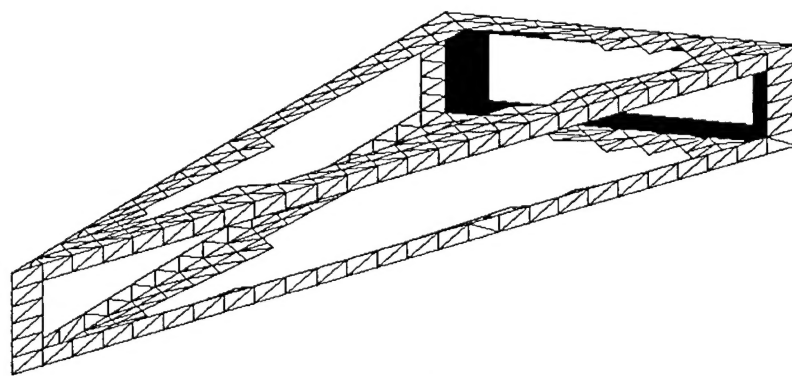


FIGURE 4. Measured and computed radar cross section of the Prism V20 object at 432 MHz, HH polarization and elevation angle 0°. The baseline MOM calculation using the un-modified IBC3D is shown for comparison. The numerical mesh of the Prism V20 object represented 2,166 total electric current unknowns in the strictly numerical MOM solution.



(a)



(b)

FIGURE 5. Exploded view of Prism V20 numerical mesh showing regions selected for MOM solution only and region to be selected for PO currents, provided they are in the lit region. (a) Flat regions selected for PO currents, (b) Edge sections reserved for numerical MOM solution.

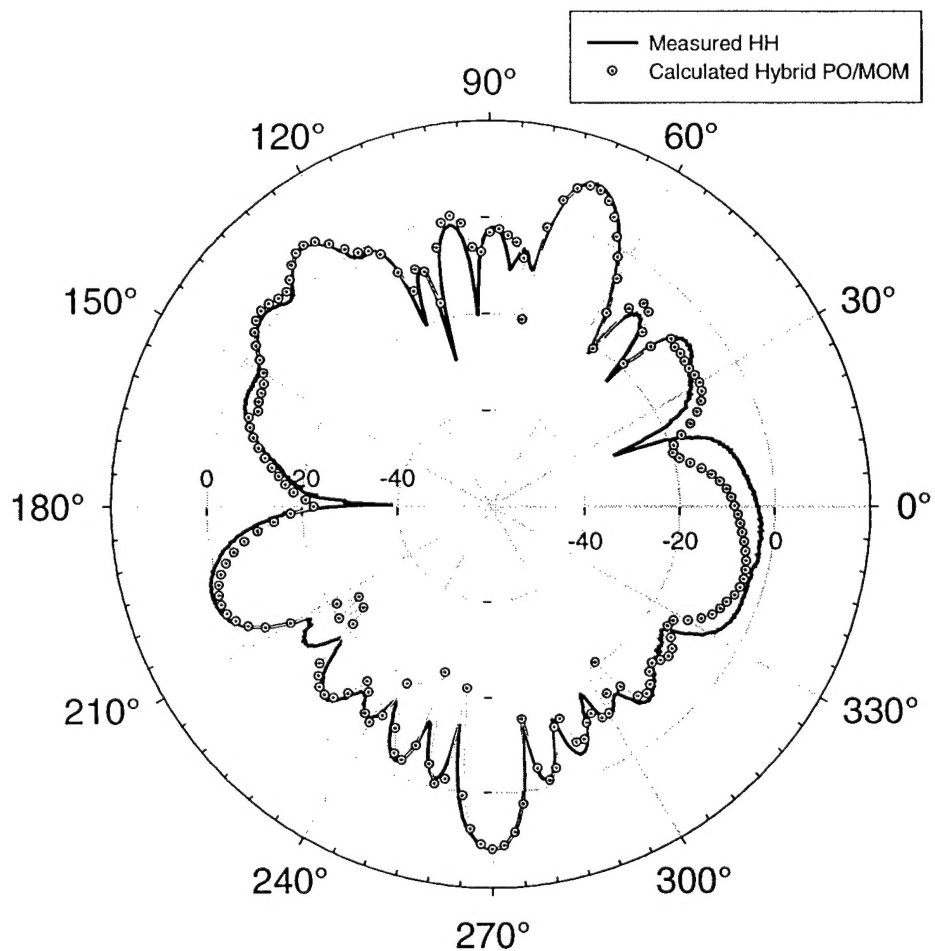


FIGURE 6. Measured and computed radar cross section of the Prism V20 object at 432 MHz, HH polarization and elevation angle 0°. The PO/MOM hybrid calculation using the modified IBC3D is shown for comparison. The agreement is good in the angular regions where the incident angle is near normal to the any of the three flat faces, 270, 70 and 140 degrees.

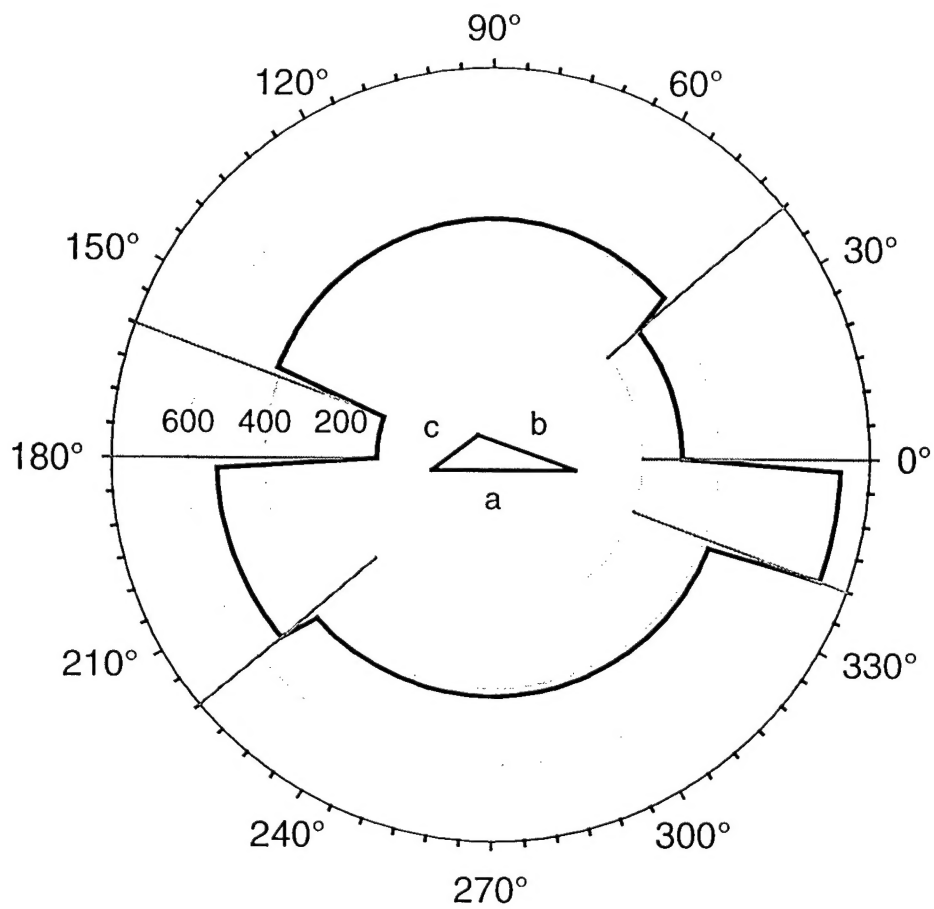


FIGURE 7. Polar plot of the number of physical optics unknowns on the Prism V20 object as a function of aspect angle. An outline of the object is inscribed in the center of the plot to illustrate the orientation of the Prism V20 flat faces. The discontinuous nature of the number of PO unknowns arises from the criteria for selecting PO edges on the body and a large number of edges meeting the criteria simultaneously. The largest number of PO edges are selected when faces 'a' and 'c' are illuminated by the incident field, the smallest when they are shadowed.